ELSEVIER

Materials Science and Engineering A284 (2000) 219–225

MATERIALS SCIENCE & ENGINEERING A

www.elsevier.com/locate/msea

# Thermal stability of nanocrystalline Ni silicides synthesized by mechanical alloying

M.K. Datta, S.K. Pabi, B.S. Murty *

*Department of Metallurgical and Materials Engineering, Indian Institute of Technology, Kharagpur 721 302, India*

Received 26 November 1999; received in revised form 4 January 2000

**Abstract**

Solid state reactions induced by mechanical alloying followed by isothermal annealing in elemental blends of Ni and Si have been studied over the entire composition range of the Ni–Si system. Above a critical crystallite size, the congruent melting phases, $\gamma$-$Ni_{31}Si_{12}$ and NiSi, become unstable and react with second phase available to form equilibrium non-congruent, $\beta_1$-$Ni_3Si$ and $\alpha$-$NiSi_2$, after isothermal annealing at 723 and 1023 K, respectively. Formation of equilibrium $\varepsilon$-$Ni_3Si_2$ has not been observed in the composition range 33–50at.% Si even after annealing at 1073 K. The results also indicate that the crystallite size of non-congruent melting phases is well above 100 nm even at the stage of their evolution, suggesting that they are probably stable only in the bulk state. The grain growth is faster for the non-congruent phases when compared to that of congruent melting compounds. The interfacial energy of the compounds plays an important role in controlling their stability and grain growth in the nanocrystalline state. 

*Keywords:* Nickel silicides; Mechanical alloying; Nanocrystalline materials; Thermal stability

## 1. Introduction

Transition metal silicides have been identified as highly promising candidates for diverse fields of application, which stems from their unique range of properties, such as high melting point, low density, low electrical resistivity and high resistance to oxidation and corrosion [1,2]. However, due to their narrow composition range and high melting points, processing of these intermetallics by conventional methods is extremely difficult. In this context, mechanical alloying (MA) which involves low temperature solid state reactions, provides an attractive alternative route for the synthesis of these intermetallics [3,4]. In addition, the feasibility of producing these intermetallics in the nanocrystalline state has widened the scope of MA.

Ni-silicides are one of the most widely studied silicide systems due to their high temperature performance and microelectronics application. Solid state reactions between Ni (crystalline) and Si (crystalline or amorphous) multilayers during annealing have been studied extensively [5–8]. Low temperature annealing of multilayers has resulted either in amorphous phase or congruent melting silicides ($\gamma$-$Ni_{31}Si_{12}$, $\delta$-$Ni_2Si$ and NiSi), whereas non-congruent melting compounds, $\beta_1$-$Ni_3Si$ and $\alpha$-$NiSi_2$, have been obtained only after isothermal annealing at 723 and 1023 K, respectively [5,6]. Recently, synthesis of nickel silicides by MA or mechanical milling has been reported by a number of investigators [9–14]. Radlanski and Calka [9] and Omuro and Miura [10], have shown that the final milled powder is a mixture of $\delta$-$Ni_2Si$ and $\gamma$-$Ni_{31}Si_{12}$ for the elemental blend of $Ni_{70}Si_{30}$. On the other hand, formation of fcc solid solution of Si in Ni has been reported by Jang et al. [11] during MA of nominal composition $Ni_{76}Si_{24}$. Recent investigations by Zhou and Bakker [12], Jang and Tsau [13] and Cho and Koch [14] on the ball milled samples of ordered $L1_2$-$Ni_3Si$, have revealed an antisite disordered structure in the early stage of milling and a phase transformation of disordered $Ni_3Si$ to fcc solid solution of Si in Ni on prolong milling. By differential scanning calorimetry (DSC) of final milled powder of ordered $Ni_3Si$, it has been identified [12–14] that the

* Corresponding author. Present address: Materials Physics Division, National Research Institute for Metals, 1-2-1 Sengen, Tsukuba 305-0047, Japan. Tel.: +81-298-592719; fax: +81-298-592701.

*E-mail address:* murty@nrim.go.jp (B.S. Murty)

0921-5093/00/$ - see front matter 
PII: S0921-5093(00)00774-7

phase restoration to ordered $Ni_3Si$ occurs around 700 K with a total heat release of 10–15 kJ $mol^{-1}$. Zhou and Bakker [12] have also reported that the activation energy for this phase restoration process is about 163 kJ $mol^{-1}$. In spite of the above reports, the thermal stability of nanocrystalline nickel-silicides synthesized by MA has not yet been clearly understood.

The present authors have recently reported [15] that only congruent melting silicides ($\gamma$-$Ni_{31}Si_{12}$, $\delta$-$Ni_2Si$ and NiSi) form in nanocrystalline state during MA in the Ni–Si system, while the non-congruent melting phases ($\beta_1$-$Ni_3Si$, $\varepsilon$-$Ni_3Si_2$ and $\alpha$-$NiSi_2$) are bypassed in the whole range of composition. The present paper reports the thermal stability of these nanocrystalline nickel silicides based on the results of isothermal annealing treatment in a wide range of compositions and thermodynamic concepts have been utilized to understand the stability of various nickel-silicides.

## 2. Experimental

Mixtures of elemental powders of Ni and Si of 99.5% purity, corresponding to nominal compositions $Ni_{100-x}Si_x$ ($x = 10$, 15, 20, 25, 28, 33, 37, 40, 45, 50, 60, 67 and 75) (Fig. 1) were subjected to milling using a high energy planetary ball mill (Fritsch Pulverisette-5). The milling was carried out at 300 rev. $min^{-1}$ for 30 h with WC milling media using a ball to powder weight ratio of 10:1. The composition of the mechanically alloyed powders was analyzed using an energy dispersive X-ray (EDX) microanalyzer, attached to a Philips CM30 transmission electron microscope (TEM). After 30 h of MA, the mechanically alloyed powders were annealed isothermally at various temperatures (573, 623, 673, 723, 773, 823, 873, 923, 973 and 1073 K) for 4 h in evacuated quartz capsules ($\sim 10^{-6}$ torr). The milled and heat-treated powders were characterized by X-ray diffraction (XRD) using a Philips 1710 X-ray diffractometer with $CoK_\alpha$ radiation. The effective crystallite size and relative strain of mechanically alloyed powders as well as heat-treated products were calculated using the Voigt function of single line method [16] after eliminating the instrumental broadening contribution. The effective crystallite size and relative strain of Ni, Si and different intermetallic phases have been calculated from their most intense peaks in the XRD patterns.

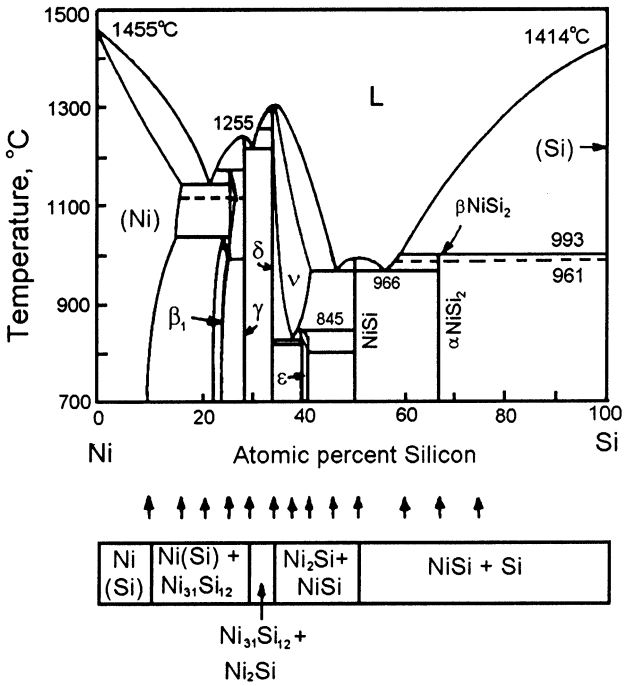


Fig. 1. Ni–Si phase diagram showing the phase fields in nanocrystalline state after MA (bar diagram).

## 3. Results

The end product compositions (analyzed by EDX microanalyzer attached to TEM) and phases formed after 30 h of MA are shown in Table 1 as a function of the initial blend composition along with the corresponding equilibrium phase(s) expected at the milled compositions. Nanocrystalline phase/phase mixtures of Ni(Si), Ni(Si) + $\gamma$-$Ni_{31}Si_{12}$, $\gamma$-$Ni_{31}Si_{12}$ + $\delta$-$Ni_2Si$, $\delta$-$Ni_2Si$ + NiSi and NiSi + Si have been obtained during MA over the composition ranges of 0–10, 10–28, 28–33, 33–50 and > 50at.% Si, respectively, after 30 h of milling [15], as shown in Fig. 1. The results clearly suggest that only congruent melting phases ($\gamma$-$Ni_{31}Si_{12}$, $\delta$-$Ni_2Si$ and NiSi) form in the nanocrystalline state ($\sim$15–25 nm) during MA and the formation of non-congruent melting phases ($\beta_1$-$Ni_3Si$, $\varepsilon$-$Ni_3Si_2$ and $\alpha$-$NiSi_2$) is bypassed even at their equilibrium phase fields. The results of the isothermal annealing of selected nominal compositions (25, 40, 67 and 75at.% Si) are presented here.

In the case of nominal composition of 25at.% Si, MA has resulted in the formation of a mixture of congruent melting compound, $Ni_{31}Si_{12}$, and fcc solid solution of Si in Ni (Ni(Si)) instead of equilibrium non-congruent melting, ordered $Ni_3Si$. Fig. 2 shows the XRD patterns of $Ni_{75}Si_{25}$ after 30 h of MA and after annealing for 4 h at 573, 623, 673, 723 and 773 K. The XRD patterns remain almost unchanged up to 673 K, except for the sharpening of the peaks due to annihilation of defects, strain relaxation and grain growth. At 723 K, a sudden change in the XRD pattern was observed, which evidenced the disappearance of $Ni_{31}Si_{12}$ and a concurrent evolution of ordered $Ni_3Si$. The transformation temperature (673–723 K) agrees well with that reported for multilayer diffusion couple experiments ($\sim$723 K) [6] and for phase restoration ($\sim$700 K) of ball milled ordered $Ni_3Si$ [12–14].

Table 1
Phases obtained after 30 h of MA and final heat treatment with their compositions and the corresponding equilibrium phases[a]

| Si content of the initial blend (at.%) | Si content after 30 h of milling (at.%) | Phases present after 30 h of MA | Phases present in final heat treated powder | Equilibrium phases at RT at milled compositions |
|---|---|---|---|---|
| 10 | 9.1 | Ni(Si) | Ni(Si) | Ni(Si) |
| 15 | 13.2 | Ni(Si)+$Ni_{31}Si_{12}$ | Ni(Si)+ord. $Ni_3Si$ | Ni(Si)+ord. $Ni_3Si$ |
| 20 | 18.2 | Ni(Si)+$Ni_{31}Si_{12}$ | Ni(Si)+ord. $Ni_3Si$ | Ni(Si)+ord. $Ni_3Si$ |
| 25 | 22.9 | Ni(Si)+$Ni_{31}Si_{12}$ | ord. $Ni_3Si$ | ord. $Ni_3Si$ |
| 28 | 25.7 | Ni(Si)+$Ni_{31}Si_{12}$ | ord. $Ni_3Si$+$\gamma$-$Ni_{31}Si_{12}$ | ord. $Ni_3Si$+$\gamma$-$Ni_{31}Si_{12}$ |
| 33 | 30.9 | $Ni_{31}Si_{12}$+$Ni_2Si$ | $\gamma$-$Ni_{31}Si_{12}$+$\delta$-$Ni_2Si$ | $\gamma$-$Ni_{31}Si_{12}$+$\delta$-$Ni_2Si$ |
| 37 | 35.1 | $Ni_2Si$+NiSi | $\delta$-$Ni_2Si$+NiSi | $\delta$-$Ni_2Si$+$\varepsilon$-$Ni_3Si_2$ |
| 40 | 37.0 | $Ni_2Si$+NiSi | $\delta$-$Ni_2Si$+NiSi | $\delta$-$Ni_2Si$+$\varepsilon$-$Ni_3Si_2$ |
| 45 | 42.7 | $Ni_2Si$+NiSi | $\delta$-$Ni_2Si$+NiSi | NiSi+$\varepsilon$-$Ni_3Si_2$ |
| 50 | 48.1 | $Ni_2Si$+NiSi | $\delta$-$Ni_2Si$+NiSi | NiSi+$\varepsilon$-$Ni_3Si_2$ |
| 60 | 58.3 | NiSi+Si | NiSi+$\alpha$-$NiSi_2$ | NiSi+$\alpha$-$NiSi_2$ |
| 67 | 65.2 | NiSi+Si | NiSi+$\alpha$-$NiSi_2$ | NiSi+$\alpha$-$NiSi_2$ |
| 75 | 73.2 | NiSi+Si | $\alpha$-$NiSi_2$+Si | $\alpha$-$NiSi_2$+Si |

[a] RT, room temperature.

The long-range order parameter, $S$, of ordered $Ni_3Si$ has been calculated to be about 0.45 at the temperature of its formation (723 K). Earlier, Zhou and Bakker [12] had identified that ordered $Ni_3Si$ starts to decompose when the $S$ value falls in the range of 0.6–0.4 during mechanical milling of ordered $Ni_3Si$. It is interesting that the reverse process observed in the present study occurs more or less at similar $S$ (i.e. 0.45) suggesting this transformation to be first order in nature. The lattice parameter of Ni(Si) before the transformation (673 K) has been calculated to be 0.3516 nm, which corresponds to a solid solution of 10at.% Si in Ni [17]. The lattice parameter of ordered $Ni_3Si$ at the onset of formation (723 K) was estimated as $\sim 0.3509$ nm, which is in good agreement with the literature value of ordered $Ni_3Si$ [17]. The above results suggest that disordered $Ni_3Si$ ($S=0$), could not be formed in the present study. From the effective free energy calculation model [15], it has been estimated that the difference between enthalpy of formation of $\gamma$-$Ni_{31}Si_{12}$ and ordered $Ni_3Si$ at 25at.% Si is about 11 kJ $mol^{-1}$, which is close to the experimental value of phase restoration of ball milled ordered $Ni_3Si$ (10–15 kJ $mol^{-1}$) measured by Zhou and Bakker [12], Cho and Koch [14] and Jang and Thau [13], while the ordering energy of $Ni_3Si$ is about 5 kJ $mol^{-1}$ [18]. Therefore, through careful examination of present and earlier works [11–14], it appears that ordered $Ni_3Si$ arises through a peritectoid type of reaction between Ni(Si) and $\gamma$-$Ni_{31}Si_{12}$ and not by reordering of disordered $Ni_3Si$.

Fig. 3 shows the grain coarsening and strain relaxation behavior of Ni(Si) and $\gamma$-$Ni_{31}Si_{12}$ phases with increasing temperature. The increase of crystallite size with temperature is very small for both Ni(Si) and $\gamma$-$Ni_{31}Si_{12}$ (from 10 and 17 nm in the as-milled state to 40 and 50 nm at 673 K for Ni(Si) and $\gamma$-$Ni_{31}Si_{12}$, respectively). Once the crystallite size of $\gamma$-$Ni_{31}Si_{12}$ reaches about 50 nm, it appears to become unstable and reacts with Ni(Si) to form equilibrium non-congruent ordered $Ni_3Si$. The results also indicate that crystallite size of ordered $Ni_3Si$ is about 135 nm at the temperature of its formation (723 K), which suggests that the grain growth is very fast for this phase and it is probably stable only in the bulk state (above 100 nm). It must be noted that the transformation temperature (673–723 K) is about 0.45–0.48$T_m$ and 0.49–0.51$T_m$ for $\gamma$-$Ni_{31}Si_{12}$ and $\beta_1$-$Ni_3Si$, respectively, which is comparable with the temperature for grain growth in conventional polycrystalline materials (0.5$T_m$). The lattice strain of Ni(Si) and $\gamma$-$Ni_{31}Si_{12}$ decreases rapidly with increasing temperature and saturates at a low value (0.2%) for $\beta_1$-$Ni_3Si$.

In the case of nominal composition of 40at.% Si, a mixture of two congruent melting compounds, $\delta$-$Ni_2Si$

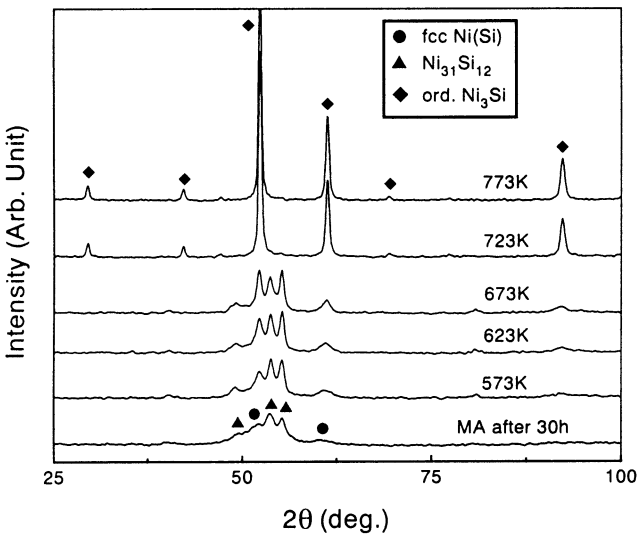


Fig. 2. XRD patterns of $Ni_{75}Si_{25}$ milled for 30 h and annealed at 573, 623, 673, 723 and 773 K for 4 h.

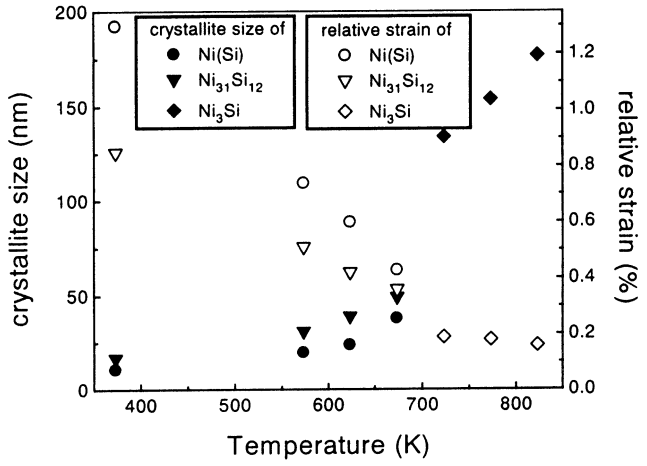


Fig. 3. Average crystallite size and relative strain of Ni(Si), $\gamma$-$Ni_{31}Si_{12}$ and $\beta_1$-$Ni_3Si$ as a function of annealing temperature for $Ni_{75}Si_{25}$.

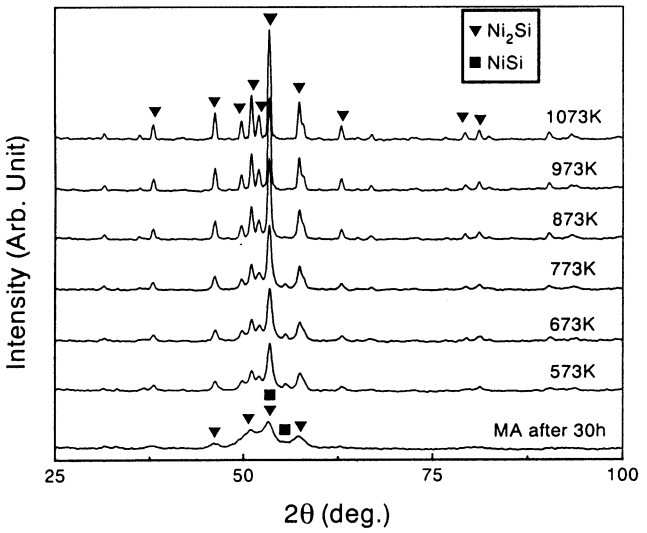


Fig. 4. XRD patterns of $Ni_{60}Si_{40}$ milled for 30 h and annealed at 573, 673, 773, 873, 973 and 1073 K for 4 h.

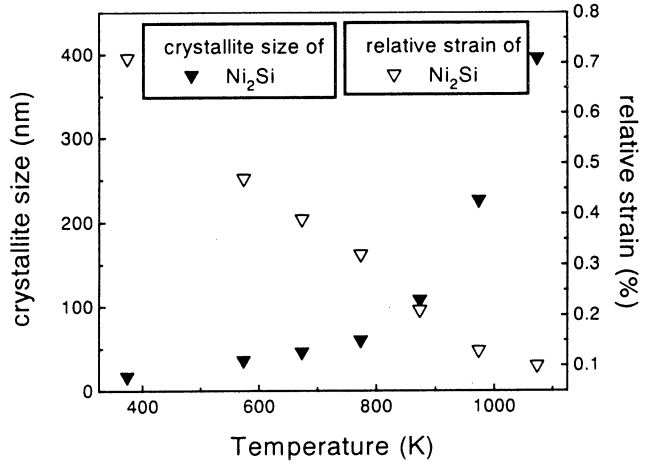


Fig. 5. Average crystallite size and relative strain of $\delta$-$Ni_2Si$ as a function of annealing temperature for $Ni_{60}Si_{40}$.

and NiSi, has been obtained on MA. However, the phase diagram shows that this composition corresponds to non-congruent melting compound $\varepsilon$-$Ni_3Si_2$. Fig. 4 compares the XRD patterns of the mechanically alloyed sample (30 h) of 40at.% Si with those annealed at 573, 673, 773, 873, 973 and 1073 K for 4 h after 30 h of MA. No trace of $\varepsilon$-$Ni_3Si_2$ peaks has been identified even after annealing up to 1073 K. It is possible that the formation of $\varepsilon$-$Ni_3Si_2$ is bypassed as reported in multilayer diffusion couple experiments [6] due to the presence of a nucleation barrier or the kinetic instability imposed by interface reaction barriers. Fig. 5 shows the variation of crystallite size and lattice strain of $\delta$-$Ni_2Si$ with temperature. The crystallite size increases very slowly up to 773 K (60 nm at 773 K in comparison to 17 nm in the as-milled state) for $\delta$-$Ni_2Si$. A substantial grain growth has been observed between 773 and 973 K (from 60 nm at 773 K to 110 and 226 nm at 873 and 973 K, respectively), which corresponds to a temperature range of $0.49–0.55T_m$, comparable with that of the grain growth in conventional polycrystalline materials ($0.5T_m$). The crystallite size of $Ni_2Si$ reached about 396 nm after annealing at 1073 K (corresponding to $0.68T_m$), suggesting that $Ni_2Si$ with small amount of NiSi is stable in bulk as well as in nanocrystalline state in the composition range 33–50at.% Si. The strain in $\delta$-$Ni_2Si$ decreases continuously with increasing temperature and reaches about 0.1% at 1073 K.

The formation mechanism of the other non-congruent melting phase, $\alpha$-$NiSi_2$, has been studied for compositions greater than 50at.% Si, which showed a mixture of NiSi and Si after 30 h MA. According to the equilibrium phase diagram, the composition ranges of 50–67 and $>67$at.% Si, correspond to the mixture of NiSi + $\alpha$-$NiSi_2$ and $\alpha$-$NiSi_2$ + Si, respectively. The XRD patterns of $Ni_{33}Si_{67}$ at different annealing temperatures (573, 673, 773, 873, 973, 1023 and 1073 K) after MA for 30 h are shown in Fig. 6. Due to the excellent epitaxy of $\alpha$-$NiSi_2$ with Si all XRD peaks of both these phases overlap, which causes difficulty in identifying the formation of $NiSi_2$. However, a close look at the XRD patterns shows that at 1023 K, the intensity of the Si peak increases suddenly. To confirm the formation of $NiSi_2$, the ratio of integrated intensity of Si (111, $2\theta = 33.17°$) and NiSi (112, $2\theta = 53.75°$) has been plotted with temperature in Fig. 7, which shows a sudden jump in the range of 973–1023 K. This could be attributed to the formation of $NiSi_2$ by a peritectoid type of reaction between Si and NiSi in this temperature range. The fact that the intensity ratio remains almost constant beyond 1023 K suggests that the reaction is complete at this temperature and that Si peaks have been replaced by $NiSi_2$ peaks. Fig. 8 shows the XRD patterns of $Ni_{25}Si_{75}$ after annealing at 573, 773, 873, 973, 1023 and 1073 K subsequent to 30 h of MA. It is very clear from Fig. 8 that NiSi peaks disappear at

1023 K which strengthens the earlier proposition in the case of 67at.% Si that Si and NiSi react to form α-$NiSi_2$ in the temperature range of 973–1023 K. This transformation temperature (973–1023 K) agrees well with multilayer diffusion couple experiments (1023 K) [6]. Thus, the reaction between Si and NiSi around 1023 K appears to lead to a mixture of α-$NiSi_2$ + NiSi and α-$NiSi_2$ + Si at the nominal compositions of 67 and 75at.% Si (milled compositions being 65 and 73at.% Si, respectively), which are the equilibrium phase mixtures at these milled compositions. Fig. 9 shows the crystallite size and lattice strain of NiSi and α-$NiSi_2$ for 67at.% Si with increase of temperature. The crystallite size of NiSi increases very slowly up to 773 K. A substantial grain growth has been observed at around

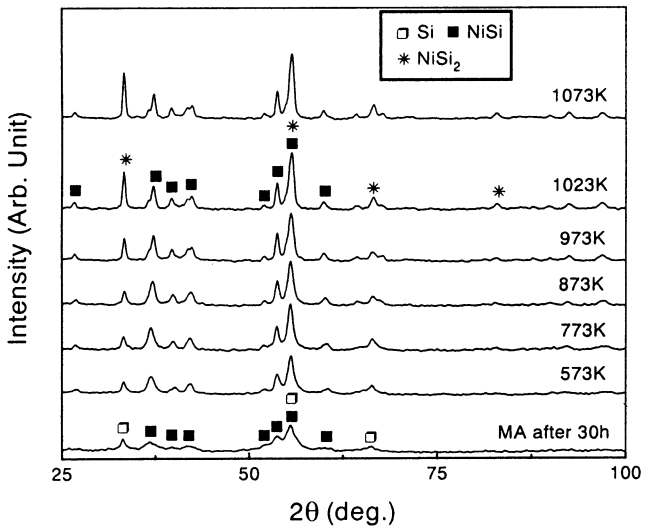


Fig. 6. XRD patterns of $Ni_{33}Si_{67}$ annealed at 573, 673, 773, 873, 973, 1023 and 1073 K for 4 h after MA for 30 h.

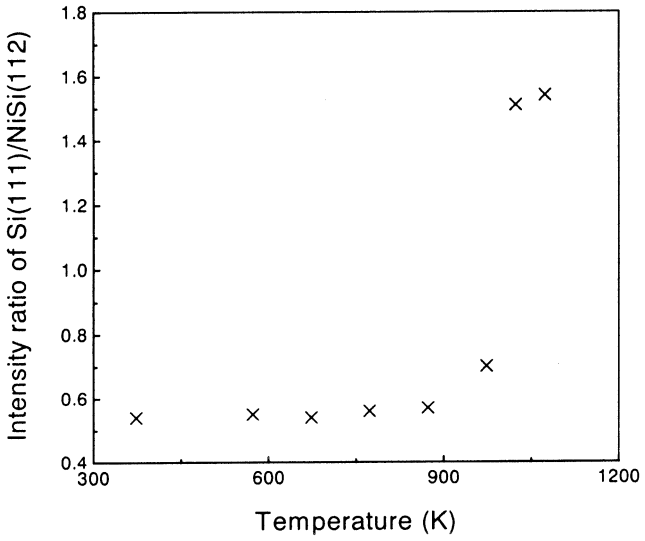


Fig. 7. Ratio of integrated intensity of Si and NiSi with temperature for $Ni_{33}Si_{67}$.

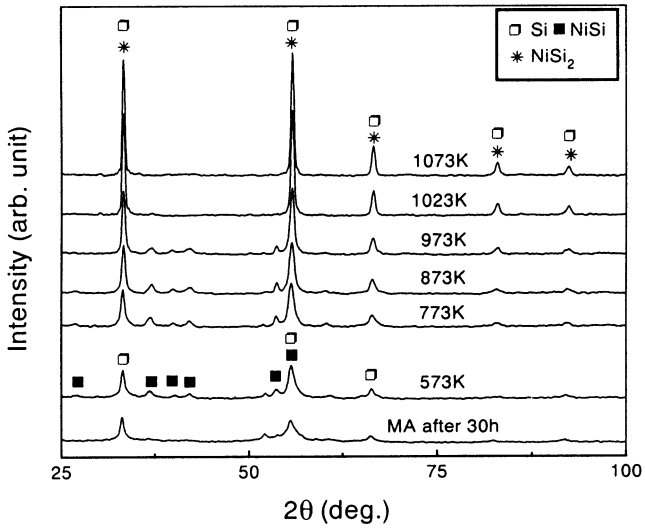


Fig. 8. XRD patterns of $Ni_{25}Si_{75}$ annealed at 573, 673, 773, 873, 973, 1023 and 1073 K for 4 h after MA for 30 h.

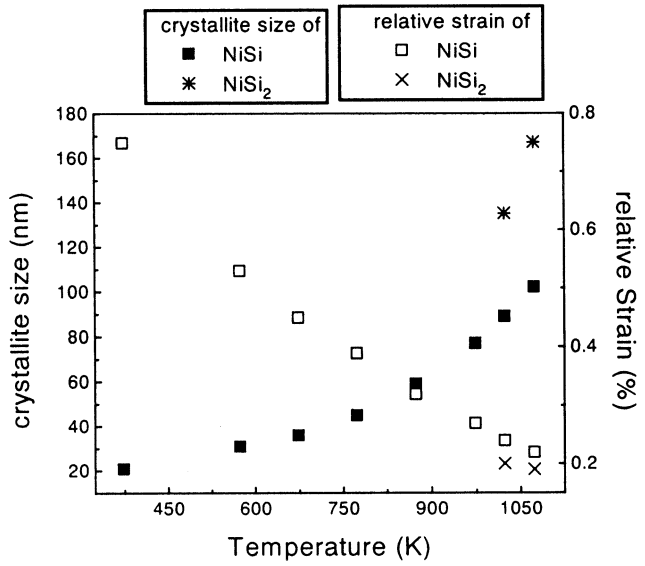


Fig. 9. Average crystallite size and relative strain of NiSi and α-$NiSi_2$ as a function of annealing temperature for $Ni_{33}Si_{67}$.

873 K, which corresponds to $0.55T_m$. Once the crystallite size of NiSi reaches about 75 nm (973 K), it reacts with Si to form equilibrium, non-congruent α-$NiSi_2$. The crystallite size of α-$NiSi_2$ is about 135 nm at the onset of its formation, suggesting that it is probably stable only in the bulk state, similar to $\beta_1$-$Ni_3Si$.

Table 1 compares the final products of isothermal annealing for all the compositions studied with those formed after MA and the equilibrium phase fields. It is very clear that except in the composition range of 33–50at.% Si, isothermal annealing has led to the restoration of equilibrium in all the compositions. The nucleation and growth of ε-$Ni_3Si_2$ in the above composition range appears to be quite sluggish even at the

highest temperature of annealing (1073 K) used in the present study.

## 4. Discussion

The results of the present work suggest that the congruent melting compounds, $\gamma$-$Ni_{31}Si_{12}$ and NiSi, are stable at non-congruent $\beta_1$-$Ni_3Si$ and $\alpha$-$NiSi_2$ phase fields, respectively in the nanocrystalline state. Once the crystallite sizes of these congruent melting phases increase beyond a critical crystallite size, they appear to become unstable and react with the second phase available, namely, Ni(Si) and Si, respectively for $\gamma$-$Ni_{31}Si_{12}$ and NiSi to form equilibrium non-congruent ordered $Ni_3Si$ and $\alpha$-$NiSi_2$, respectively. The results also indicate that the crystallite sizes of the non-congruent melting $\beta_1$-$Ni_3Si$ and $\alpha$-$NiSi_2$ are well above 100 nm even at the stage of their evolution, which suggests that grain growth is very fast for these phases and that these phases are probably stable only in the bulk state.

It is interesting to note that while the non-congruent melting compounds $\beta_1$-$Ni_3Si$ and $\alpha$-$NiSi_2$ have formed during isothermal annealing in the present study, the formation of another non-congruent melting compound $\varepsilon$-$Ni_3Si_2$ could not be observed even after annealing at 1073 K for 4 h in the composition range of 33–50at.% Si, in which it exists under equilibrium conditions. It is interesting to note that in the case of the formation of $\beta_1$-$Ni_3Si$ and $\alpha$-$NiSi_2$, one of the reacting species is a solid solution or a pure metal, namely, Ni(Si) or Si, respectively, while in case of $\varepsilon$-$Ni_3Si_2$, both the reacting species are intermetallic compounds. It is expected that the mass transport is more difficult in the case of intermetallic compounds and hence the nucleation and growth of $\varepsilon$-$Ni_3Si_2$ at the interface between NiSi and $\delta$-$Ni_2Si$ is probably quite difficult. Also, the phase diagram shows that $Ni_3Si_2$ forms by a low temperature peritectoid reaction between $\delta$-$Ni_2Si$ and NiSi at 1118 K on cooling. It is well known that peritectoid reactions are quite sluggish and hence the temperature and time used in the present study are probably insufficient for the reaction between $\delta$-$Ni_2Si$ and NiSi to yield $\varepsilon$-$Ni_3Si_2$.

The solid state reaction between Ni and Si to form congruent melting phase in nanocrystalline state and the formation of non-congruent melting phases in the bulk state (above 100 nm) at non-congruent phase fields can be understood through thermodynamic considerations. The thermodynamic condition for phase 1 to be stable in a bulk material over phase 2 is that $G_1 < G_2$ ($G$, Gibb's free energy per unit volume). In the case of nanocrystalline materials, the contribution of the interfacial energy term ($G^{int}$) to the free energy cannot be neglected. In a nanocrystalline state, phase 2 may become stable if $G_1 + G_1^{int} > G_2 + G_2^{int}$ [19]. The above condition implies that below a critical crystallite size, the phases with lower interfacial energy become energetically favored. The congruent melting phases, formed by energetic processes, generally exhibit low energy interfaces characterized by coherent or semicoherent interfaces [15,20], whereas non-congruent melting phases, formed by assembly of kinetic processes, exhibit high-energy configuration of high angle grain boundary [15,20]. Therefore, it is expected that the rate of increase of overall free energy ($G + G^{int}$) of non-congruent melting phases will be higher than the congruent melting phases with refinement of crystallite size. Thus, below a critical crystallite size, it is expected that the congruent phase will be stable over non-congruent phases, whereas above this critical crystallite size the non-congruent phases will be stable in their phase fields as the interfacial energy contribution to the free energy can be neglected. Thus, the nanocrystalline state appears to favor congruent melting compounds, whereas the non-congruent melting phases will be formed at their phase fields in the bulk state as observed in the present study.

The grain growth behavior of congruent and non-congruent phase could also be explained by considering the interfacial energy. The grain growth in polycrystalline materials is driven by the decrease of interfacial energy and hence total energy of the system. According to the well-known Gibbs–Thomson [21] equation regarding the grain growth process in conventional polycrystals, it is expected that the driving force for grain growth increases with a reduction of grain size, which might be extremely large for the nanometer-sized grains even at room temperature. However, contrary to the expectation, experimental observations indicate that most nanocrystalline materials of either elements or compounds, synthesized by various methods, exhibit inherent grain size stability up to reasonably high temperatures [20,22].

The grain size stability in the nanocrystalline materials has so far been found to be closely related to the structural characteristics of the material, such as the grain size and its distribution, grain morphologies, triple junctions, presence of second phase, porosity in the sample and so on [20,22,23]. Some new structural information of the nanocrystalline materials, e.g. a decrease in the interfacial energy with grain refinement [20,24] and the lattice distortion of the nanometer-sized crystallites [20,25,26] also plays an important role in controlling the grain growth in nanocrystalline materials. The present results show that the increase of crystallite size with temperature of congruent melting compounds, $\gamma$-$Ni_{31}Si_{12}$, $\delta$-$Ni_2Si$ and NiSi, is very small, whereas the crystallite size of non-congruent melting compounds, $\beta_1$-$Ni_3Si$ and $\alpha$-$NiSi_2$, is above 100 nm even at the onset of their formation. Grain growth in conventional materials is considered to be controlled by

atomic diffusion at the grain boundary. The grain boundary diffusion coefficient of an element depends on the angle of misorientation at the grain boundaries. Low energy grain boundaries (low angle grain boundary) are generally more closely packed and consequently will present lower diffusivities, whereas high energy grain boundaries (high angle grain boundaries), particularly along their tilt axis, are much more open and thus present easy paths for grain boundary diffusion, resulting in faster grain growth. Therefore, it is expected that the grain growth of congruent melting phases will be slower due to their lower interfacial energy. On the other hand, as the interfacial energy of non-congruent melting compounds is much higher, these compounds are susceptible to rapid grain growth as observed in the present study. Other possible reasons for sluggish grain growth in the congruent melting compounds may include solute drag due to the presence of a lower density second phase at the grain boundary [27], triple junction [28] and lattice distortion from equilibrium configuration [29].

## 5. Conclusions

The congruent melting compounds, $\gamma$-$Ni_{31}Si_{12}$ and NiSi, obtained by MA in the phase fields of non-congruent melting compounds ($\beta_1$-$Ni_3Si$ and $\alpha$-$NiSi_2$), are stable in the nanocrystalline state and become unstable above a critical crystallite size leading to the formation of the latter.

Non-congruent melting compounds, $\beta_1$-$Ni_3Si$ and $\alpha$-$NiSi_2$, form during isothermal annealing of mechanically alloyed samples at 723 and 1073 K, respectively. Formation of $\varepsilon$-$Ni_3Si_2$ could not be observed even after isothermal annealing at 1073 K in the composition range of 33–50at.% Si.

The non-congruent melting compounds ($\beta_1$-$Ni_3Si$ and $\alpha$-$NiSi_2$) are stable only when their crystallite size is above 100 nm.

The congruent melting compound with the highest melting point, $\delta$-$Ni_2Si$, is stable both in the nanocrystalline and bulk (crystallite size of $\sim$400 nm) state in the phase field of non-congruent melting $\varepsilon$-$Ni_3Si_2$.

It has been identified that the interfacial energy of congruent and non-congruent melting phases in the nanocrystalline state plays an important role in controlling the grain size stability of nanocrystalline materials.

## References

[1] K.S. Kumar, C.T. Liu, JOM 45 (1993) 28.
[2] S.P. Muraka, Silicides for VLSI Applications, Academic Press, New York, 1983.
[3] B.S. Murty, S. Ranganathan, Int. Mater. Rev. 43 (1998) 101.
[4] F.H. Froes, C. Suryanarayana, K. Russel, C.G. Li, Mater. Sci. Eng. A192/A193 (1995) 612.
[5] R. Pretorius, T.K. Maris, C.C. Theron, Mater. Sci. Eng. 10 (1993) 1.
[6] J.W. Mayer, S.S. Lau, Electronic Materials Science: for Integrated Circuits in Si and GaAs, Macmillan, New York, 1990, pp. 306–309.
[7] L.A. Clevenger, C.V. Thompson, J. Appl. Phys. 68 (1990) 1325.
[8] W.H. Wang, H.Y. Bai, W.K. Wang, Mater. Sci. Eng. A179/A180 (1994) 22.
[9] A.P. Radlinski, A. Calka, Mater. Sci. Eng. A134 (1991) 1376.
[10] K. Omuro, H. Miura, Appl. Phys. Lett. 60 (1992) 1433.
[11] J.S.C. Jang, C.H. Tsau, W.D. Chen, P.Y. Lee, J. Mater. Sci. 33 (1998) 265.
[12] G.F. Zhou, H. Bakker, Acta Metall. Mater. 42 (1994) 3009.
[13] J.S.C. Jang, C.H. Tsau, J. Mater. Sci. 28 (1993) 982.
[14] Y.S. Cho, C.C. Koch, J. All. Comp. 194 (1993) 287.
[15] M.K. Datta, S.K. Pabi, B.S. Murty, J. Appl. Phys., in press.
[16] T.H. de Keijser, J.I. Langford, E.I. Mittemeijer, A.B.P. Vogels, J. Appl. Crystallogr. 15 (1982) 308.
[17] W.B. Pearson, A Handbook of Lattice Spacing and Structures of Metals and Alloys, Pergamon, Oxford, 1958, p. 786.
[18] D.I. Potter, in: R. Holland, L. Mansur, D.I. Potter (Eds.), Phase Stability during Irradiation, TMS-AIME, Warrendale, PA, 1981, p. 521.
[19] V.G. Grayznov, L.I. Trusov, Prog. Mater. Sci. 37 (1993) 289.
[20] K. Lu, Mater. Sci. Eng. R16 (1996) 161.
[21] P.G. Sewmon, Transformation in Metals, McGraw-Hill, New York, 1969, p. 300.
[22] C. Suryanarayana, Int. Mater. Rev. 40 (1995) 41.
[23] V.V. Novikov, Scripta Mater. 39 (1999) 945.
[24] K. Lu, R. Ruck, B. Predel, Scripta Metall. Mater. 28 (1993) 1387.
[25] M.K. Datta, S.K. Pabi, B.S. Murty, J. Mater. Res, submitted.
[26] X.D. Liu, K. Lu, H.Y. Zhang, Z.Q. Hu, J. Phys. Condens. Matter. 6 (1994) L497.
[27] K. Boylan, D. Ostrander, U. Erb, G. Palumbo, K.T. Aust, Scipta Metall. Mater. 25 (1991) 2711.
[28] G. Palumbo, U. Erb, K.T. Aust, Scripta Metall. Mater. 24 (1990) 2347.
[29] M.K. Datta, S.K. Pabi, B.S. Murty, unpublished data.